

## Production and fate of transparent exopolymer particles in the ocean

Oliver Wurl,<sup>1,2</sup> Lisa Miller,<sup>1</sup> and Svein Vagle<sup>1</sup>

Received 6 June 2011; revised 26 September 2011; accepted 17 October 2011; published 30 December 2011.

[1] The production and fate of transparent exopolymer particles (TEP) have been investigated in various oceanic regions (tropical, temperate, and polar), from the sea surface microlayer (SML) to the deep ocean. Accumulation of TEP within the mixed layer was observed even in the absence of phytoplankton blooms, indicating abiotic processes are important in TEP production. The abiotic TEP aggregation rates measured in the tropical and temperate North Pacific and the Arctic Ocean averaged between 8 and 12  $\mu\text{mol C L}^{-1} \text{d}^{-1}$ . Depth profiles from under sea ice in the Arctic revealed the highest TEP concentrations, potentially released by sympagic algal activity at the bottom of the sea ice. The aggregation rates in the SML, the interfacial layer between the ocean and atmosphere, were generally enhanced over those in the bulk surface waters by factors of 2 to 30. This finding further strengthens a developing consensus on the gelatinous nature of the SML, which will also affect microbial life, light penetration, and surface wave properties. We present a conceptual model implying that abiotic aggregation is an important factor for TEP production in the ocean, in particular in sea surface microlayers, while consumption by zooplankton and protists recycle TEP, providing a new pool of dissolved precursor material. Overall, TEP is recycled within the water column through heterotrophic grazing and degradation, providing a new pool of TEP precursor materials, while enhanced aggregation rates of TEP in the SML indicates the importance of this thin surface film in the marine carbon cycle.

**Citation:** Wurl, O., L. Miller, and S. Vagle (2011), Production and fate of transparent exopolymer particles in the ocean, *J. Geophys. Res.*, 116, C00H13, doi:10.1029/2011JC007342.

### 1. Introduction

[2] The formation and sinking of biogenic particles mediate vertical mass fluxes, influence optical properties and drive elemental cycling in the ocean, ultimately driving both primary and secondary production and contributing to global climate control. Whereas marine scientists have focused primarily on particle production by phytoplankton growth and aggregation, particle formation by the abiotic assembly of organic macromolecules has been largely neglected.

[3] Transparent exopolymer particles (TEP), ubiquitous and abundant in the ocean, are gels possessing strong surface active properties [Passow, 2002]. These particles are mainly formed by abiotic coagulation of dissolved carbohydrates [Chin *et al.*, 1998] excreted by phytoplankton communities. Due to their surface active properties, or “stickiness,” TEP act as a glue matrix for other solid particles (i.e., detritus), forming larger aggregates (marine snow) and playing an important role in the export of carbon from the surface to the

deep ocean [Passow *et al.*, 2001]. In addition, they represent an essential food source for the benthos and microorganisms residing within the water column below the euphotic zone. Earlier studies have shown that TEP concentrations decrease with depth [Engel *et al.*, 2004], implying at least some consumption by bacteria during sinking.

[4] If unballasted, TEP are positively buoyant and ascend toward the surface to accumulate in the sea surface microlayer (SML), contributing a gelatinous composition to this interfacial film between the ocean and atmosphere [Wurl and Holmes, 2008; Wurl *et al.*, 2009]. Cunliffe and Murrell [2009] reviewed and discussed the finding of the gelatinous nature of the SML within the context of the bacterioneuston, e.g., bacterial communities residing in the SML. The SML is known to concentrate, to varying degrees, many chemical compounds (i.e., carbohydrates, proteins, and lipids), in particular those that are surface active (surfactants), modifying the chemical and physical properties of the sea surface. For example, the gelatinous, or biofilm-like, composition of the SML may also have significant effects on the penetration of light and UV radiation. For example, Elasmri and Miller [1999] showed that biofilm matrices adsorb UV radiation to a significant extent. High amounts of surface active substances in the SML also cause wave damping, affecting light reflection and, consequently, penetration.

<sup>1</sup>Institute of Ocean Sciences, Fisheries and Oceans Canada, Sidney, British Columbia, Canada.

<sup>2</sup>Now at Department of Ocean, Earth, and Atmospheric Sciences, Old Dominion University, Norfolk, Virginia, USA.

[5] It has been hypothesized that particle aggregation may be enhanced in the SML due to coagulation of the concentrated dissolved organic matter. *Williams* [1967] wrote: “Detritus derived from the surface films [SML] undoubtedly contributes some fractional part to the particulate organic matter in the euphotic zone and possibly to deep water particulates.” Earlier *Riley* [1963] concluded, “Formation on the sea surface seems the only likely explanation for sheet-like aggregates of the order of meter or two in lengths that have been observed occasionally,” and although we now know that pelagic invertebrates also contribute to the formation of such aggregates, processes at the sea surface almost certainly contribute, as well. In his seminal paper, *Carlson* [1993] suggested various processes that potentially favor the transformation from dissolved to particulate organic matter, including heterogeneous precipitation, phase changes of surface molecules and repetitive compression and dilation of the sea surface by wave motion. However, to date, none of these speculations have been confirmed.

[6] The aim of this study was to investigate the production and fate of TEP in different regions of the ocean (tropical, temperate and polar). We have investigated the formation rates and accumulation of TEP in the euphotic zone and how these relate to water column stratification, primary production and sea surface conditions. Furthermore, we have investigated TEP production in the SML to test the hypothesis of enhanced particle aggregation in this interfacial boundary layer. The results are tied together with a new conceptual model for the TEP cycle in the ocean.

## 2. Methods

### 2.1. Study Areas

[7] Water samples were collected as part of the Radiance in a Dynamic Ocean (RaDyO) project onboard the *R/V Kilo Moana* off Hawaii, on an Arctic research cruise onboard the *CCGS Amundsen* as part of the Canadian ArcticNet program, from the *CCGS J.P. Tully* as part of the Line P and La Perouse programs (see Line P web page provided by Fisheries and Oceans Canada) and from a research ice camp hosted by the Catlin Arctic Survey in the high Canadian Arctic. The ice base was located at N 78° 46.2' W 104° 43.3' in Deer Bay, off Ellef Ringnes Island. The water depth at the site of the ice base is unknown but greater than 230 m, as measured with the winch wire. The sampling areas and times represent different trophic states, as well as climatic conditions (Figure 1). Physical and biological features of the sampling areas are presented in Table 1.

### 2.2. Sample Collection

[8] For this study we collected 16 water column profiles (from the SML down to as deep as 4200 m), plus 12 paired samples from the SML and bulk water at a depth of 1 m. Samples from the SML were collected using a glass plate sampler [*Harvey and Burzell*, 1972] from the bow of a small boat as described in detail by *Wurl et al.* [2011]. The glass plate was immersed vertically and withdrawn gently at a speed of 5–6 cm s<sup>-1</sup> (as consistently as conditions allowed). Adhering water was removed by wiping the plate with a squeegee into a sample container. The SML thickness collected by this withdrawal rate is about 50 μm [*Carlson*, 1982] and consistent with experimentally determined SML

thicknesses of 50 ± 10 μm using pH microelectrodes [*Zhang et al.*, 2003]. Subsurface samples from 1 m were collected with a 120 mL syringe and weighted polypropylene tubing. Separate subsurface samples from 1 and 8 m were also collected with the syringe and tubing and were filtered onto GF/F filters (47 mm diameter; 500–2000 mL) for chlorophyll-a (Chl-a) analysis. All samples were stored cool during sampling operations. All sampling equipment was washed with 10% HCl and rinsed with ultra pure water prior to use.

[9] Samples from the Catlin ice camp were collected with a Niskin bottle and a hand-operated winch through an ice hole (sea ice thickness about 1.6 m). The ice hole was located about one nautical mile from the camp and about five nautical miles from the nearest shore in water more than 200 m deep. A tent was built over the ice hole to facilitate sampling without freezing and to help keep the hole open between sampling events (typically every 2–3 days), thereby minimizing any disturbances of the underlying water column immediately prior to sampling. Ice slurry from the water surface was removed with a sieve prior to sampling.

[10] At the water column sampling locations (Figure 1), temperature, salinity, fluorescence and dissolved oxygen concentration were measured by CTD casts. In the Pacific, the mixed layer depth (MLD) was estimated as the depth at which temperature differed from the surface by 0.1°C. *Steiner et al.* [2007] showed good agreement between this criterion and MLD derived from modeled turbulent kinetic energy at station P. In the Arctic Ocean (ARC and CAT stations), the MLD was estimated as the depth at which density differed from the surface by 0.125 kg m<sup>-3</sup>. The depth of the euphotic layer ( $z_{Eu}$ ) was estimated from the Secchi disk depth ( $z_{Sec}$ ) as  $z_{Eu} = 1.79 z_{Sec}$  [*Preisendorfer*, 1986].

[11] At the time of SML collection, averaged wind speed was measured using a handheld weather station (Kestrel, Model 3000). We also noted the formation of surface slicks in the sampling area by visual observation. During slick conditions, the concentration of surface active organic materials in the SML exceeds some presently unknown threshold value, and the microlayer becomes visible as smooth gray spots or stripes due to capillary wave damping.

### 2.3. Chemical Analysis

[12] The TEP concentrations were measured spectrophotometrically according to a dye-binding assay [*Engel*, 2009]. Subsamples (10 to 200 mL) of SML and subsurface water were filtered onto 0.4 μm polycarbonate filters under low vacuum (<100 mm Hg) immediately after collection, stained with 500 μL alcian blue solution (0.02 g alcian blue in 100 mL of acetic acid solution of pH 2.5), and rinsed twice with 1 mL of DI water. Each filter was soaked for 2 h in 6 mL of 80% sulfuric acid (H<sub>2</sub>SO<sub>4</sub>) to dissolve the dye and then the absorbance of the solution was measured at 787 nm in a 1 cm cuvette. The acidic polysaccharide xanthan gum (Sigma Aldrich) was used as a standard. The detection limit and precision were 4 μg xanthan gum equivalents (Xeq) L<sup>-1</sup> and better than 13%, respectively. Concentrations in μg Xeq L<sup>-1</sup> have been converted to carbon (μg C L<sup>-1</sup>) using the conversion factor of 0.63 [*Engel*, 2004], which is based on a reanalysis of multiple investigations using different phytoplankton cultures and therefore, is appropriate for our study of diverse marine environments.

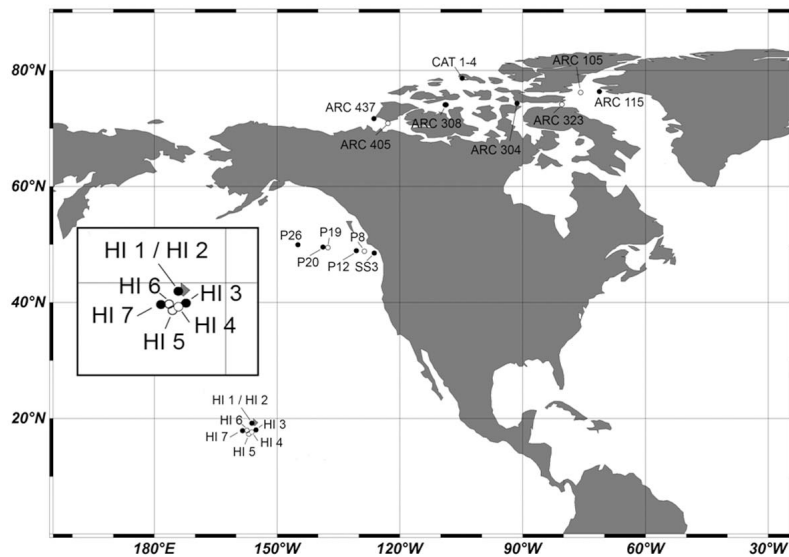


**Figure 1.** Sampling sites off Vancouver Island (SS), along Line P (P), offshore Hawaii (HI), in the north-west passage (ARC), and at the Catlin ice base (CAT). Black dots represent microlayer and full water column sampling, and white dots represent only microlayer and subsurface water (1 m depth). Note that, for clarity, only the big island of Hawaii is shown.

[13] The concentrations of total dissolved carbohydrates were determined spectrophotometrically using 2,4,6-tripyridyl-s-triazine (TPTZ) as a complexing reagent [Mykkestad *et al.*, 1997]. Subsamples for TDC were filtered over  $0.2 \mu\text{m}$  polycarbonate filters prewashed in 10% HCl. Filtrates were stored in precombusted ( $450^\circ\text{C}$  for 5 h) screw cap test tubes at  $-20^\circ\text{C}$  for up to 4 weeks. Prior to analysis, the samples were hydrolyzed with 0.85 M  $\text{H}_2\text{SO}_4$  (final concentration) at  $100^\circ\text{C}$  for 24 h to convert polysaccharides

to monosaccharides [Borch and Kirchman, 1997]. Concentrations of monosaccharides were determined with the same approach in nonhydrolyzed samples, and the concentrations of dissolved polysaccharides (PCHO) were determined by the concentration difference between total carbohydrates and monosaccharides. The procedure typically has a precision better than 7%, based on samples analyzed in triplicate.

[14] Primary production was computed using the Vertical Generalized Production Model (VGPM) [Behrenfeld and

**Table 1.** Physical and Biological Features of Sampling Sites for Water Column Profiles

Sampling Date	Latitude/ Longitude (deg)	MLD <sup>a</sup> (m)	Chl-a <sup>b</sup> ( $\mu\text{g L}^{-1}$ )		PP <sup>b</sup> ( $\text{g m}^{-2} \text{d}^{-1}$ )		Depth of Max. FL <sup>c</sup> (m)	Sea Ice Coverage (Visual Observation)	
			1 m	8 m	1 m	8 m			
<i>North Pacific</i>									
SS 3	3 Jun 2009	51.25/−129.35	8.9	1.54	1.72	2.53	n.a.	25.0	
P 12	9 Jun 2009	48.97/−130.67	12.4	0.42	0.43	1.99	0.40	35.6	
P 20	11 Jun 2009	49.57/−138.73	11.0	0.46	0.37	1.65	0.26	37.5	
P 26	14 Jun 2009	50.00/−145.00	12.8	0.30	0.31	1.79	0.26	41.3	
<i>Offshore Hawaii</i>									
HI 1	27 Aug 2009	19.25/−156.13	21.3	0.53	0.46	0.81	1.04	125.6	
HI 2	28 Aug 2009	19.25/−155.97	22.0	0.63	0.38	1.19	0.86	114.9	
HI 3	1 Sep 2009	17.77/−156.07	39.1	0.52	0.47	0.48	0.44	114.2	
HI 7	9 Sep 2009	18.00/−158.42	31.4	0.42	0.47	0.71	0.66	147.0	
<i>Arctic Ocean</i>									
ARC 437	14 Oct 2009	71.78/−126.49	29.0	0.34	0.31	0.03	0.03	36.4	0%
ARC 308	19 Oct 2009	74.10/−108.83	13.0	0.14	0.15	0.01	0.01	23.9	100%
ARC 304	23 Oct 2009	74.31/−91.33	26.0	1.68	1.61	0.15	0.14	5.7	100%
ARC 115	29 Oct 2009	76.33/−71.19	20.0	0.71	0.57	0.01	0.01	6.3	0%
CAT 1	25 Mar 2010	78.77/−104.72	12.0	6.40	5.67	n.a.	n.a.	n.a.	100%
CAT 2	18 Apr 2010	78.77/−104.72	12.5	4.20	6.07	n.a.	n.a.	n.a.	100%
CAT 3	22 Apr 2010	78.77/−104.72	14.0	6.90	7.80	n.a.	n.a.	n.a.	100%
CAT 4	24 Apr 2010	78.77/−104.72	13.0	6.57	5.67	n.a.	n.a.	n.a.	100%

<sup>a</sup>Mixed layer depth.

<sup>b</sup>Chlorophyll-a (Chl-a) and primary production (PP) as reported by Wurl *et al.* [2011]. Chl-a data at CAT stations from 3m and 10 m depth.

<sup>c</sup>Maximum fluorescence (FL) reading from conductivity-temperature-depth sensor package.

**Table 2.** Average Concentrations of TEP ( $\mu\text{mol C L}^{-1}$ ) and PCHO ( $\mu\text{mol C L}^{-1}$ ), and dTEP/dt Formation Rates ( $\mu\text{mol C L}^{-1} \text{d}^{-1}$ ) Above and Below the Mixed Layer Depth (MLD) to 250 m

	Sampling Date	TEP		PCHO		dTEP/dt	
		Above MLD	Below MLD	Above MLD	Below MLD	Above MLD	Below MLD
<i>North Pacific</i>							
SS 3	3 Jun 2009	16.0	4.9	10.8	17.8	5.9	4.6
P 12	9 Jun 2009	41.2	14.6	12.8	5.4	14.7	3.4
P 20	11 Jun 2009	8.0	6.4	8.1	14.0	2.8	4.4
P 26	14 Jun 2009	7.0	3.2	17.1	6.8	8.0	0.9
Average $\pm$ SD		18.1 $\pm$ 15.9	7.3 $\pm$ 5.1	12.2 $\pm$ 3.8	11.0 $\pm$ 5.9	7.9 $\pm$ 5.0	3.3 $\pm$ 1.7
<i>Offshore Hawaii</i>							
HI 1	27 Aug 2009	37.9	10.9	21.2	23.9	26.8	12.7
HI 2	28 Aug 2009	11.6	8.4	23.2	10.1	10.8	4.8
HI 3	1 Sep 2009	3.9	2.5	25.7	22.0	7.9	5.2
HI 7	9 Sep 2009	3.3	<2.5	10.9	8.9	2.0	1.2
Average $\pm$ SD		14.2 $\pm$ 16.3	5.8 $\pm$ 4.6	20.3 $\pm$ 6.5	16.2 $\pm$ 7.8	11.9 $\pm$ 10.6	6.0 $\pm$ 4.8
<i>Arctic Ocean</i>							
ARC 437	12 Oct 2009	11.8	6.1	10.9	19.6	3.8	5.9
ARC 308	19 Oct 2009	5.3	5.0	2.9	6.3	0.6	1.1
ARC 304	23 Oct 2009	6.6	5.2	11.4	11.8	3.0	2.6
ARC 115	29 Oct 2009	18.1	13.4	17.7	16.2	11.8	7.0
Average $\pm$ SD		10.5 $\pm$ 5.8	7.4 $\pm$ 4.0	10.7 $\pm$ 6.1	13.5 $\pm$ 5.8	4.8 $\pm$ 4.9	4.2 $\pm$ 2.8
CAT 1	25 Mar 2010	6.5	4.3	11	1.8	3.4	0.3
CAT 2	18 Apr 2010	74.3	43.2	12.0	5.9	23.5	7.6
CAT 3	22 Apr 2010	28.2	16.6	12.1	9.4	12.5	5.0
CAT 4	24 Apr 2010	27.4	17.4	10.8	17.7	9.0	11.9
Average $\pm$ SD		33.8 $\pm$ 28.7	19.8 $\pm$ 16.5	12.2 $\pm$ 1.1	8.2 $\pm$ 5.8	12.0 $\pm$ 8.4	5.6 $\pm$ 4.0

Falkowski, 1997] as described by Wurl *et al.* [2011]. For Chl-a determination, filters were extracted into 10 mL of acetone for 24 h at 4°C, with sonication for the first five minutes. Spectrophotometric analysis was conducted according to *Strickland and Parsons* [1972], substituting the equation from *Jeffrey and Humphrey* [1975]. Chlorophyll-a data for the ARC and CAT stations were provided by M. Gosselin (ISMER, Université du Québec à Rimouski) and H. Findlay (Plymouth Marine Laboratory, UK), respectively.

#### 2.4. Validation of Glass Plate Techniques for Collection of TEP

[15] The possibility that TEP from the bulkwater could stick to the glass plate, and thereby appear to be part of the microlayer pool, was of a concern, and we investigated the potential for such a bias. First, we filled acid-washed glass bottles (soda lime glass similar to the glass plate) with seawater of known TEP concentration. After an exposure of ten seconds, equivalent to the time required for a single dip with the glass plate, the water was discharged. Three ml of Alcian blue were added to the bottles to stain the TEP adhering to the walls. Bottles were rotated gently to ensure all surfaces are stained. Staining occurs immediately. Bottles were rinsed with several mL of DI water to remove excessive staining solution. Six ml of 80% sulphuric acid were added to the bottles and extracted for two hours on a rolling table. Control bottles that had not been exposed to seawater were treated similarly. Second, we loaded ten mL of DI water onto horizontal glass plates, which had been used for sampling. After several seconds, the DI water was wiped off with a squeegee directly into a filter funnel for TEP filtration and staining as described in the previous section. This procedure was repeated thrice for each side of the glass plate.

Third, the used glass plates from the previous experiment were stained with about ten ml of alcian blue solution, rinsed with DI water, and the stained matter was extracted by carefully rinsing the plate with six mL of 80% sulphuric acid. This experiment did not allow an extraction time of two hours, but shorter extraction time may remove the majority of the stained matter efficiently [*Passow and Alldredge*, 1995].

[16] The amount of TEP extracted from the glass bottle wall was on average  $10 \pm 4\%$  of the concentration of TEP in the seawater used to fill the bottles. A similar observation was reported by *Ortega-Retuerta et al.* [2009b] and indicates that a small fraction of bulkwater TEP may adhere to the glass plate during sampling. Triplicate experiments on rinsing and wiping (with a squeegee) glass plates that had been exposed to seawater with DI water gave absorbances of  $0.161 \pm 0.013$ ,  $0.199 \pm 0.024$  and  $0.210 \pm 0.024$  after filtration of the rinses ( $n = 6$  for each experiment) and extraction of TEP-stained filter membranes. The measured absorbances were insignificantly different ( $p = 0.2644$ , unpaired t test) from the absorbance of pure DI water ( $abs = 0.209 \pm 0.030$ ,  $n = 4$ ). The results indicate that any TEP stuck to the glass plate is not removed by wiping off adhering water. Final staining of the used glass plates yielded an average absorbance of  $0.271 \pm 0.077$ , indicating a small quantity of TEP on the plate, similar to our glass bottle experiments and those of *Ortega-Retuerta et al.* [2009b]. Overall, our results indicate quick adherence of glass surfaces with TEP without any significant effect on the integrity of adhering SML sample. Some TEP from the microlayer may adhere to the plate more persistently too, but based on our bottle experiments, only a small fraction of TEP seems to stick on the glass surface. We also routinely

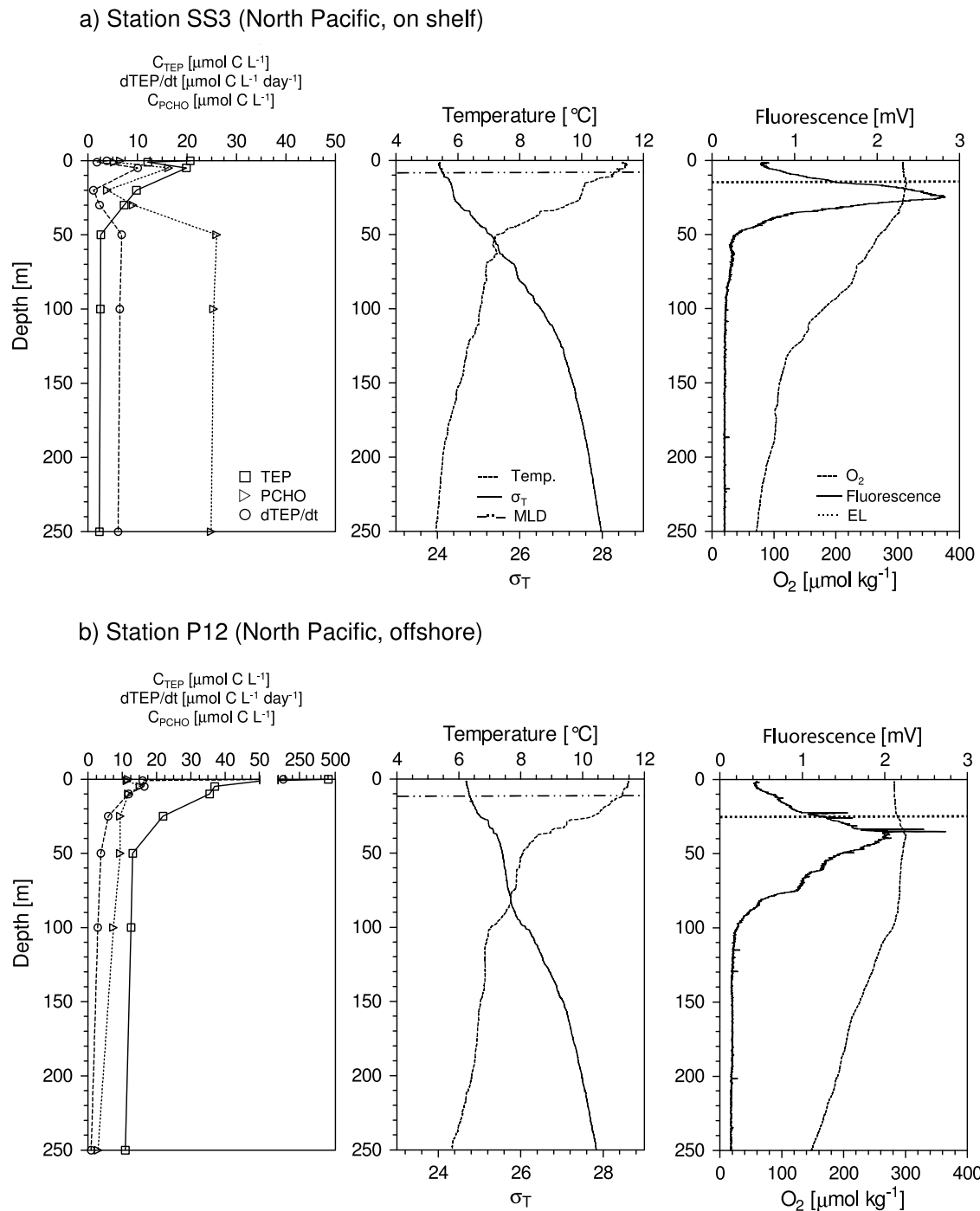


**Figure 2.** Vertical profiles of TEP ( $C_{\text{TEP}}$ ), dissolved polysaccharides ( $C_{\text{PCHO}}$ ), TEP formation rates ( $d\text{TEP}/dt$ ), temperature, density ( $\sigma_T$ ), fluorescence (uncalibrated), and oxygen concentration during cruises in the subpolar North Pacific. Stations (a) SS 3 (on shelf) and (b) P 12 (offshore). MLD, mixed layer depth; EL, euphotic layer depth.

condition the glass plate sampler with 10–15 dips before collecting samples.

## 2.5. Aggregation Model

[17] Aggregation by physical coagulation requires that primary polymers and particles collide by Brownian motion or advection and then stick together. Coagulation theory as established by *Smoluchowski* [1917] has recently been

applied to describe aggregation of marine particles [*Burd and Jackson, 2009*]:

$$\frac{d\text{TEP}}{dt} = \alpha_{\text{PCHO}}\beta_{\text{PCHO}}[\text{PCHO}]^2 + \alpha_{\text{TEP}}\beta_{\text{TEP}}[\text{PCHO}][\text{TEP}] \quad (1)$$

where  $[\text{PCHO}]$  is the concentration of dissolved polysaccharide [ $\mu\text{mol C L}^{-1}$ ],  $[\text{TEP}]$  is the concentration of TEP

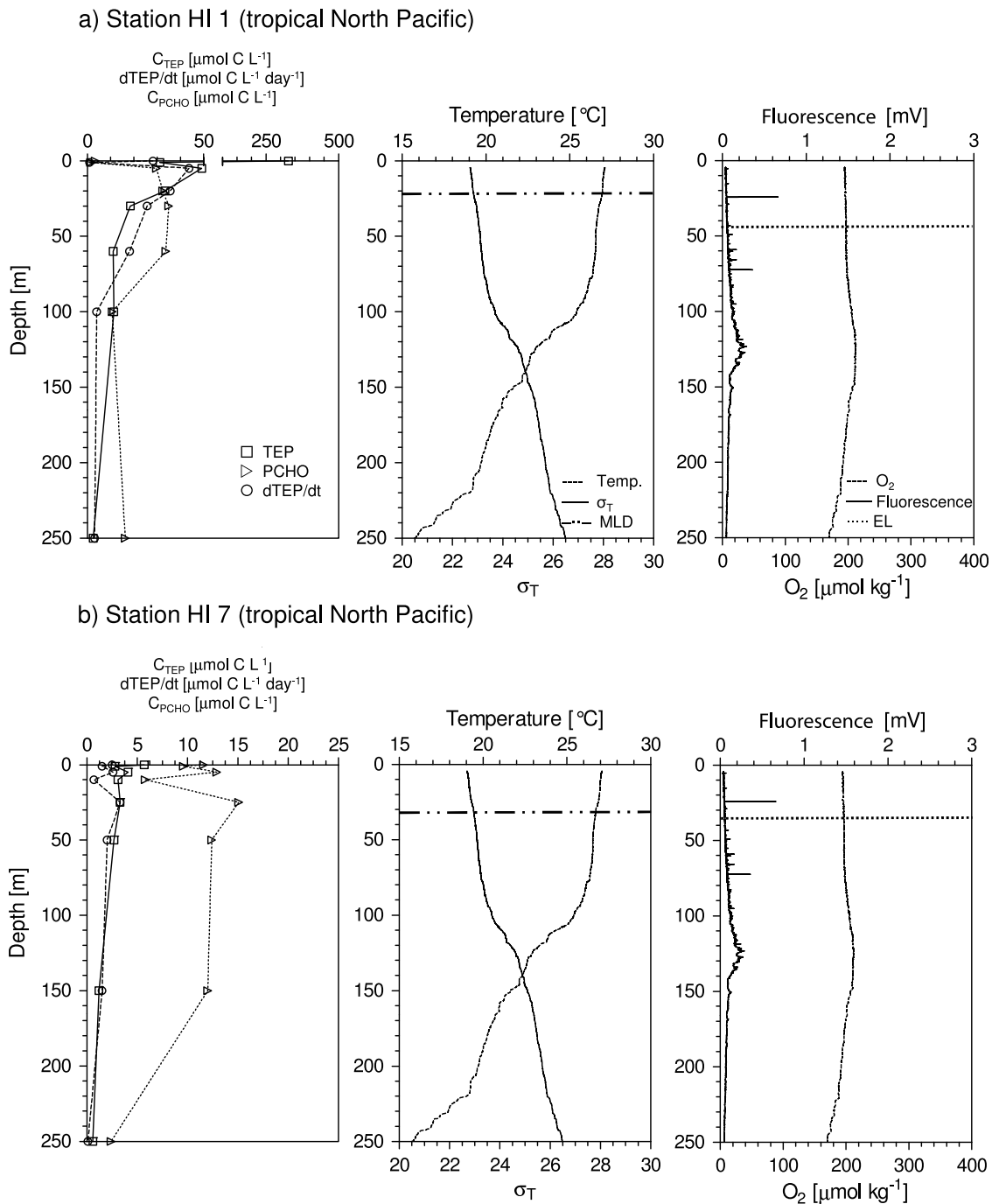


**Figure 3.** Vertical profiles of TEP ( $C_{\text{TEP}}$ ), dissolved polysaccharides ( $C_{\text{PCHO}}$ ), TEP formation rates ( $d\text{TEP}/dt$ ), temperature, density ( $\sigma_T$ ), fluorescence (uncalibrated), and oxygen concentration in the tropical North Pacific, off Hawaii. Stations (a) HI 1 (25 km offshore Hawaii Island) and (b) HI 7 (300 km offshore Hawaii Island). Bottom depth was greater than 1000 m for both stations. MLD, mixed layer depth; EL, depth of euphotic layer.

[ $\mu\text{mol C L}^{-1}$ ],  $\alpha_{\text{PCHO}}$  is the self attachment probability of PCHO,  $\alpha_{\text{TEP}}$  is the attachment probability between PCHO-TEP and  $\beta_{\text{PCHO}}$  and  $\beta_{\text{TEP}}$  are the carbon-specific collision kernels (collision frequency functions).

[18] Engel *et al.* [2004] showed, during a large-scaled mesocosm study, that such a model is adequate to describe the carbon transfer from dissolved polysaccharides (PCHO)

to TEP. Thoms [2006] discussed the parameterization of the model in detail.

[19] Here, we use the carbon-specific collision kernel according to Engel *et al.* [2004] as  $\beta_{\text{PCHO}} = 0.86 \text{ L } \mu\text{mol}^{-1} \text{ d}^{-1}$  and  $\beta_{\text{TEP}} = 0.064 \text{ L } \mu\text{mol}^{-1} \text{ d}^{-1}$ . We also used an attachment probability,  $\alpha_{\text{PCHO}}$ , of 0.00087, which was determined in mesocosm studies [Engel *et al.*, 2004] and is consistent

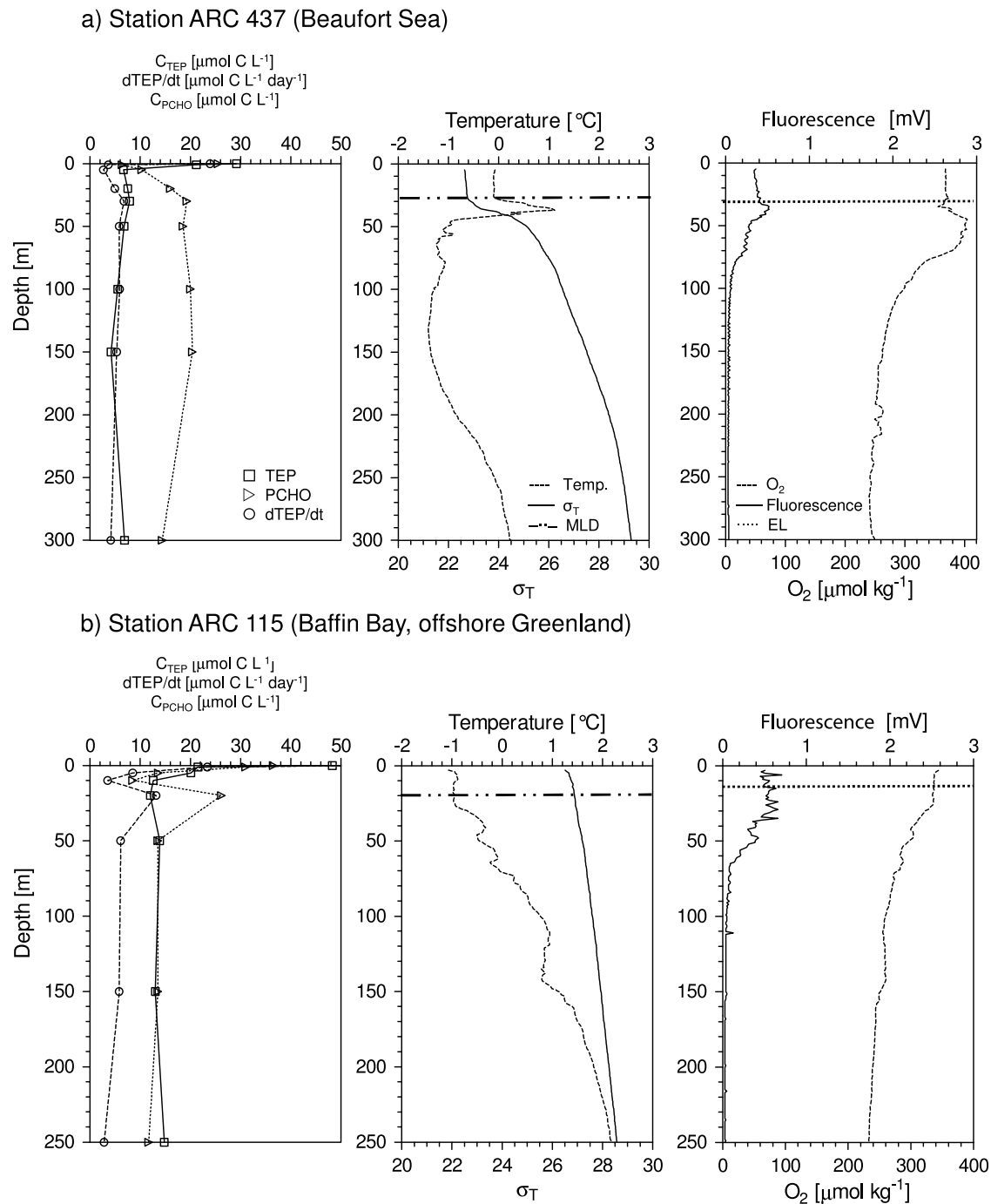


**Figure 4.** Vertical profiles of TEP ( $C_{\text{TEP}}$ ), dissolved polysaccharides ( $C_{\text{PCHO}}$ ), TEP formation rates ( $d\text{TEP}/dt$ ), temperature, density ( $\sigma_T$ ), uncalibrated fluorescence, and oxygen concentration in the southern Canadian Archipelago. Stations (a) ARC 437 and (b) ARC 115. MLD, mixed layer depth; EL, depth of euphotic layer.

with previous estimates of  $\alpha_{\text{PCHO}} < 0.001$  [Wells and Goldberg, 1992]. Attachment probability  $\alpha_{\text{PCHO-TEP}}$  can vary between 0.1 and 1 depending on bloom conditions and stage [Engel, 2000], and we used the model value of 0.4 from Engel et al. [2004]. The attachment probability may vary considerably among the different oceanic regions, and the aggregation rates in Table 2 can only be considered rough estimates. However, we anticipate smaller biases between attachment probabilities at different depths within

each station, where the TEP should be derived from the same sources, e.g., the phytoplankton communities.

## 2.6. Data Analysis

[20] Statistical analyses of the data set were performed using Graphpad PRISM Version 5.1. Differences, null hypothesis testing and correlation were considered to be significant when  $p < 0.05$ . We tested hypotheses with parametric or nonparametric tests, as stated. The data were log

















